Entanglement Structure and Information Protection in Noisy Hybrid Quantum Circuits

Shuo Liu,[1] Ming-Rui Li,[1] Shi-Xin Zhang,[2,*] and Shao-Kai Jian[3,†]
[1]*Institute for Advanced Study, Tsinghua University, Beijing 100084, China*
[2]*Tencent Quantum Laboratory, Tencent, Shenzhen, Guangdong 518057, China*
[3]*Department of Physics and Engineering Physics, Tulane University, New Orleans, Louisiana 70118, USA*

(Received 8 January 2024; revised 23 February 2024; accepted 13 May 2024; published 13 June 2024)

In the context of measurement-induced entanglement phase transitions, the influence of quantum noises, which are inherent in real physical systems, is of great importance and experimental relevance. In this Letter, we present a comprehensive theoretical analysis of the effects of both temporally uncorrelated and correlated quantum noises on entanglement generation and information protection. This investigation reveals that entanglement within the system follows $q^{-1/3}$ scaling for both types of quantum noises, where q represents the noise probability. The scaling arises from the Kardar-Parisi-Zhang fluctuation with effective length scale $L_{\text{eff}} \sim q^{-1}$. More importantly, the information protection timescales of the steady states are explored and shown to follow $q^{-1/2}$ and $q^{-2/3}$ scaling for temporally uncorrelated and correlated noises, respectively. The former scaling can be interpreted as a Hayden-Preskill protocol, while the latter is a direct consequence of Kardar-Parisi-Zhang fluctuations. We conduct extensive numerical simulations using stabilizer formalism to support the theoretical understanding. This Letter not only contributes to a deeper understanding of the interplay between quantum noises and measurement-induced phase transition but also provides a new perspective to understand the effects of Markovian and non-Markovian noises on quantum computation.

DOI: 10.1103/PhysRevLett.132.240402

Introduction.—The competition between unitary evolution and nonunitary monitored measurements gives rise to a dynamical phase transition known as the measurement-induced phase transition (MIPT) [1–21]. The entanglement within the system undergoes a transition from a volume-law phase to an area-law phase as the measurement probability increases. Theoretical understanding of MIPT [11,14] reveals its connection to the order-disorder transition of a classical spin model through the mapping between the hybrid quantum circuit and an effective statistical model. Building upon this theoretical understanding, MIPT has been extensively investigated in various systems [22–52].

The entanglement structure and information protection are intricately connected [7,8,53–56]. For a noiseless monitored random circuit in a volume law phase (also dubbed as error-resilient phase), the encoded information will remain in the system for an infinitely long time. However, in real experiments, inevitable quantum noise from the environment can disrupt entanglement within the system. [16]. From the entanglement perspective, it has been demonstrated that quantum noise can be treated as a symmetry-breaking field in the effective statistical model, resulting in a single area-law entanglement phase and the disappearance of MIPT with infinitesimal noise strength q [57–62]. Nevertheless, investigations on the information protection capacity in noisy hybrid quantum circuits are rare and strongly required, especially necessitating the identification of a characteristic timescale for information protection, because noise errors are more general and common than measurement errors on quantum devices for quantum error correction.

While temporally correlated measurements in MIPT have been explored [63,64], understanding of the distinction and connection between temporally uncorrelated and correlated quantum noises in MIPT setups remain elusive. In this Letter, we investigate quantum noises with distinct temporal correlations in monitored circuits from both entanglement and information perspectives and primarily concentrate on the latter. The temporally uncorrelated noise can be regarded as the Markovian limit, and the correlated noises correspond to the strong non-Markovian limit [65]. We not only provide a thorough theoretical understanding of the same area law $q^{-1/3}$ scaling from the entanglement perspective in the original volume law phase of MIPT but also propose a steady state information protection setup where the timescales of information protection reveal the distinctions between the effects of temporally correlated and uncorrelated quantum noises. The theoretical prediction for this timescale is crucial for a better understanding of the effects of quantum noises on information protection and is potentially relevant for quantum error corrections and quantum error mitigations [66–70].

To quantify the entanglement of the mixed states generated by the noisy hybrid quantum circuits [71,72], we use the mutual information [73] between the left and right half chains, defined as $I_{A:B} = S_A + S_B - S_{AB}$, where S_α is the von Neumann entropy of region α. Compared to the logarithmic entanglement negativity which is a measure of entanglement for mixed states [74–83], mutual information shows qualitatively similar behaviors and provides a more intuitive understanding within the framework of the statistical model [62,84]. In terms of the corresponding effective statistical model, as shown in Supplemental Material (SM) [85], S_α is expressed as the free energy difference of a classical spin model with specific boundary conditions. The presence of temporally correlated noises induces an effective length scale $L_{\text{eff}} \sim q^{-1}$ and the free energy scaling can be analytically obtained from the Kardar-Parisi-Zhang (KPZ) theory directly [84,92–97] with L_{eff}, leading to $q^{-1/3}$ scaling [62,85]. However, the extension of KPZ understanding becomes challenging in the presence of temporally uncorrelated noises with random space-time locations. We provide analytical solutions for the mechanism of $q^{-1/3}$ scaling for the latter case.

More importantly, although the effects of noises with different temporal correlations are indistinguishable from the entanglement perspective, the information protection timescales of the steady states can reveal the distinctions. With temporally correlated noise, the $q^{-2/3}$ timescale emerges as the average height of the domain wall in the statistical model. This scaling is given by KPZ theory with $L_{\text{eff}} \sim q^{-1}$ and the wandering exponent $\chi = 2/3$. The temporally uncorrelated noise is more subtle as the encoded information itself can modify the domain wall configuration in the statistical model, resulting in the $q^{-1/2}$ scaling for information protection. This scaling draws an interesting analogy between the hybrid circuits setup and the Hayden-Preskill protocol for black holes [98]. We also validate the theoretical predictions with extensive numerical results from the large-scale stabilizer circuit simulation.

Setup.—We consider a one-dimensional system with L d-qudits under the hybrid evolution with brick-wall random 2-qudit unitary gates in the presence of the projective measurements with probability p_m and the quantum noises with probability q. Different quantum channels can be employed to model quantum noise, yielding qualitatively similar results [85], while unital and nonunital quantum channels induce very different consequences in variational quantum algorithms [99]. We focus on the region $p_m < p_m^c$, where p_m^c corresponds to the MIPT critical point. The initial state is chosen as a product state $|0\rangle^{\otimes L}$ and each 2-qudit gate is independently drawn from the Haar ensemble (or from a random 2-qubit Clifford ensemble in numerical simulation). The space-time locations of the projective measurements and temporally uncorrelated quantum noises are random as shown in Fig. 1(a). In contrast, only the spatial locations of temporally correlated quantum noises are random, i.e., the locations of quantum noise show a stripe pattern in the time direction as shown in Fig. 1(b). This is the strongest limit of non-Markovianity,

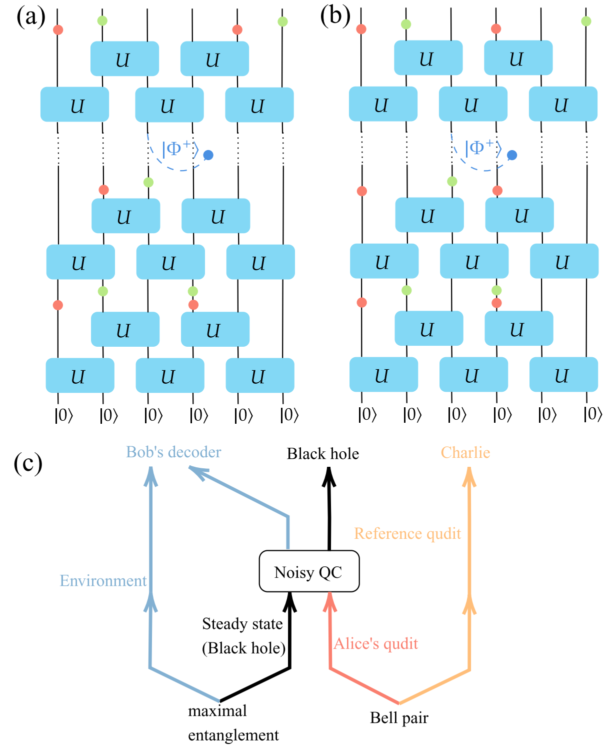

FIG. 1. Circuit diagram in the presence of temporal uncorrelated (a) and temporal correlated (b) quantum noises (red circles). The initial state is $|0\rangle^{\otimes L}$ and the projective measurements are represented by green circles. After the system reaches the steady state, a reference qudit (blue circle) is maximally entangled with the middle qudit via forming a Bell pair to encode one-qudit information. (c) shows the corresponding diagram of the Hayden-Preskill protocol. The steady state can be regarded as a black hole and Alice throws one-qudit information into the black hole to destroy it. The timescale of information protection corresponds to the time required for Bob to decode the information from collecting the qudits released by Hawking radiation.

where the noise occurrence correlation at any two different time slices at the same spatial position is constant 1.

We calculate the von Neumann entropy S_α and mutual information $I_{A:B}$ in the steady states where $I_{A:B}$ saturates and remains constant to reveal entanglement structures. We note that the time required to reach the steady state is $O(q^{-1})$ and size independent [100], differing from that of MIPT without noises. To examine the capabilities of information protection, after reaching the steady state, a reference qudit (R) is maximally entangled with the middle qudit of the system by forming a Bell pair to encode one-qudit quantum information as shown in Fig. 1, see SM for details [85]. Subsequently, we measure the mutual information $I_{AB:R}$ between the system qudits and the reference qudit to study the timescale for information protection.

Statistical model.—We introduce the mapping between the hybrid quantum circuit and the effective statistical model (see SM [85] for more details). To calculate the von Neumann entropy S_α from the free energy of the effective statistical model, S_α is expressed as $S_\alpha = \lim_{n\to 1} S_\alpha^{(n)} = \lim_{n\to 1}[1/(1-n)]\mathbb{E}_{\mathcal{U}} \log[\mathrm{tr}\rho_\alpha^n/(\mathrm{tr}\rho)^n]$, where $\mathbb{E}_{\mathcal{U}}$ represents the average over random two-qudit unitary gates, ρ_α is the reduced density matrix of region α, and $S_\alpha^{(n)}$ is the nth order Renyi entropy given by $S_\alpha^{(n)} = [1/(1-n)]\mathbb{E}_{\mathcal{U}} \log\{\mathrm{Tr}[(C_\alpha \otimes I_{\bar{\alpha}})\rho^{\otimes n}]/\mathrm{Tr}[(I_\alpha \otimes I_{\bar{\alpha}})\rho^{\otimes n}]\}$, where C and I are cyclic and identity permutations in n copies replicated Hilbert space, respectively. The average of the logarithmic function can be evaluated with the help of the replica trick [101,102], $S_\alpha = \lim_{\substack{k\to 0\\ n\to 1}}[1/k(1-n)] \log\{Z_\alpha^{(n,k)}/Z_0^{(n,k)}\} = \lim_{\substack{k\to 0\\ n\to 1}}[1/k(n-1)] [F_\alpha^{(n,k)} - F_0^{(n,k)}]$, where $Z^{(n,k)}$ corresponds to the partition function of a ferromagnetic spin model in the triangular lattice obtained by averaging over the random two-qudit unitary gates. We note that $[1/k(n-1)]F^{(n,k)}$ is independent of (n,k) and thus the limit can be safely taken. At each site of the triangular lattice, the degrees of freedom are formed by the permutation-valued spins σ defined on the permutation group S_{nk} [85]. The time runs from the bottom to the top in this effective spin model. The von Neumann entropy is represented as the free energy difference for the spin model with different top boundary conditions: $\mathbb{C}_\alpha \otimes \mathbb{I}_{\bar{\alpha}}$ and $\mathbb{I}_\alpha \otimes \mathbb{I}_{\bar{\alpha}}$ for $Z_\alpha^{(n,k)}$ and $Z_0^{(n,k)}$, respectively, where $\mathbb{C} = C^{\otimes k}$ and $\mathbb{I} = I^{\otimes k}$. The bottom boundary is free due to the initial product state and therefore $Z_0^{(n,k)} = d^0$ and $F_0^{(n,k)} = 0$ [85]. In the following discussion, we focus on the most dominant spin configuration in the large d limit, meaning that the partition function $Z^{(n,k)}$ corresponds to the weight of the dominant spin configuration.

In the absence of quantum noises and measurements, $Z_{AB}^{(n,k)}$ is d^0 because the dominant spin configuration is that all the spins are $\mathbb{C}$. Thus, $S_{AB} = 0$ consistent with the fact that the steady state is pure. However, a domain wall separating regions $\mathbb{C}$ and $\mathbb{I}$ with unit energy $|\mathbb{C}| = k(n-1)$ is formed due to the fixed top boundary condition, which is unique because of the unitary constraint [103,104]. Consequently, $F_\alpha^{(n,k)} = |\mathbb{C}|L_A$ and thus $S_A = L_A$ obeys a volume law.

In terms of the statistical model, the quantum noises act as a magnetic field pining in the direction $\mathbb{I}$ [57–61] and thus the weight of the spin configuration above for $F_{AB}^{(n,k)}$ with bulk spins in $\mathbb{C}$ is proportional to $d^{-qLT|\mathbb{C}|}$ and it is not favored anymore. Instead, quantum noises can relax the unitary constraints and induce other possible spin configurations. We leave the randomness of the locations of noises as a quenched disorder and show how to find the dominant spin configuration for each given trajectory of temporally uncorrelated quantum noises. As indicated in Fig. 2(b), spins remain $\mathbb{C}$ until the reversed evolution encounters a quantum noise $N(x_1, t_1)$. Spins inside the downward light cone of this quantum noise will change from $\mathbb{C}$ to $\mathbb{I}$ while other spins are unchanged. Other quantum noises inside the light cone of $N(x_1, t_1)$ do not affect the spin configuration because the spins are already in the $\mathbb{I}$ domain, while another quantum noise outside the light cone, e.g., $N(x_2, t_2)$, will also change the spins within its respective backward light cone from $\mathbb{C}$ to $\mathbb{I}$. Consequently, the domain wall separating regions $\mathbb{C}$ and $\mathbb{I}$ is formed by the boundary of light cones as shown in Fig. 2(b) and can be regarded as a combination of many small domain walls with an effective length scale $L_{\mathrm{eff}} \sim q^{-1}$ determined by the average distance between adjacent quantum noises.

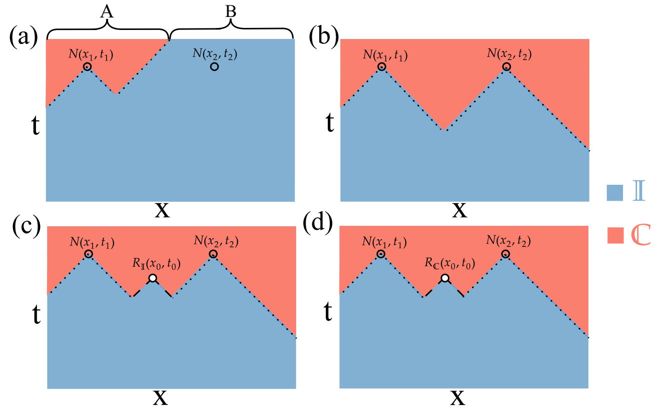

FIG. 2. The schematic dominant spin configurations: the upper panel is related to entanglement generation while the lower panel is related to information protection setup with extra Bell pair forming at (x_0, t_0). x axis and y axis correspond to spatial and time dimensions, respectively. Different colors represent the different classical spin configurations in the statistical model. N and R represent the location for quantum noise and the Bell pair, respectively. Other quantum noises within the $\mathbb{I}$ domain are not shown. (a) shows the dominant spin configuration for $F_A^{(n,k)}$. The midpoint on the top boundary will change the length scale of the domain wall near it. (b) shows the dominant spin configuration for $F_{AB\cup R}^{(n,k)}$. (c),(d) show the dominant spin configurations for $F_{AB}^{(n,k)}$ and $F_{AB\cup R}^{(n,k)}$ where spin freedom at (x_0, t_0) are fixed to $\mathbb{I}$ and $\mathbb{C}$, respectively. In the presence of measurements, the domain wall will fluctuate away from its original path.

In the presence of the projective measurements, we also leave the randomness of the space-time locations as a quenched disorder. The projective measurements can be treated as random Gaussian potential and cause the fluctuation of the domain wall away from its original respective path. The free energy can be obtained by KPZ theory with $L_{\mathrm{eff}} \sim q^{-1}$ and is consistent with the volume law entropy for the hybrid circuit [85]. Although there are quantum noises present below the original domain wall with an average height q^{-1}, the average height of the fluctuated domain wall is $q^{-2/3}$ given by the KPZ theory with $L_{\mathrm{eff}} \sim q^{-1}$ and thus we can neglect the effects of these quantum noises on the fluctuation of the domain wall. For the mutual information $I_{A:B}$, the bulk terms proportional to the subsystem size cancel out, but the boundary term from the free energy of the domain wall near the midpoint is crucial because the effective length scale for $S_{A(B)}$ has been changed as shown in Fig. 2(a), resulting in

$$I_{A:B}(q) \sim q^{-1/3}. \quad (1)$$

The theoretical prediction can be straightforwardly extended to temporally correlated quantum noise: it can be treated as emergent new boundaries that directly induce an effective length scale $L_{\mathrm{eff}} \sim q^{-1}$ [85].

Furthermore, we consider the abilities of information protection in the steady state in the presence of quantum noises. One qudit information is encoded into the steady state by forming a Bell pair between a reference qudit and a middle qudit at (x_0, t_0) of the system, see Fig. 1. The encoded information can be measured by the mutual information between the system AB and the reference qudit R

$$I_{AB:R}(t,q) = S_{AB}(t,q) + S_R(t,q) - S_{AB\cup R}(t,q). \quad (2)$$

Because the reference qudit and the middle qudit form a Bell pair, in the corresponding statistical model, the spin at position (x_0, t_0) is determined by the top boundary condition of the reference qudit. We also use R to represent this Bell pair, which is fixed to $\mathbb{I}$, $\mathbb{C}$, and $\mathbb{C}$ for S_{AB}, S_R, and $S_{AB\cup R}$, respectively.

Although the scalings of entanglement for temporally uncorrelated and correlated quantum noises are the same, the timescales of information protection are different. The dominant spin configuration for $F_R^{(n,k)}$ is where all the spins are $\mathbb{I}$ except the spin R fixed to $\mathbb{C}$, therefore, S_R is constant with contribution from the bubble created by $R_{\mathbb{C}}$. For the temporally correlated quantum noises, the dominant spin configurations for $F_{AB}^{(n,k)}$ and $F_{AB\cup R}^{(n,k)}$ change when the spin R crosses the domain wall [85]. Therefore, the timescale is given by the average height of the domain wall which is q^{-1} and $q^{-2/3}$ without and with monitored measurements.

On the contrary, for the temporally uncorrelated quantum noises, R can act similarly to quantum noise and change the spins inside its light cone from $\mathbb{C}$ to $\mathbb{I}$ as shown in Figs. 2(c) and 2(d). Therefore, the domain wall configuration has been modified and the timescale of information protection does not correspond to the height of the domain wall. A detailed analysis based on the statistical model is given in SM [85]. This information protection process can also be understood as a Hayden-Preskill protocol [98] as shown in Fig. 1(c). The steady state can be regarded as a black hole formed long ago that is maximally entangled with the environment, which is under the control of Bob. To destroy her recorded one-qudit information, which is maximally entangled with a reference qudit of Charlie, Alice throws it into the black hole. The quantum noise channels can be regarded as Hawking radiation to the environment. The Hayden-Preskill protocol tells us that the environment, i.e., Bob, only needs slightly more than one qudit from the Hawking radiation to decode Alice's information. Therefore, the timescale of information protection corresponds to the time required for a quantum noise with probability q to appear in the light cone of the encoded information with area $O(t^2)$, and hence the timescale is $q^{-1/2}$ [85]. The presence of measurements will not alter the qualitative arguments above. Therefore, the timescales of information protection for temporally correlated and uncorrelated quantum noises in MIPT are $q^{-2/3}$ and $q^{-1/2}$, respectively. We can also apply statistical model understanding to the noiseless case, where the information can be protected by the subsystem of monitored circuits ($p_m < p_m^c$) forever or with timescale $L_{\mathrm{sub}}^{2/3}$ for $L_{\mathrm{sub}} > L/2$ or $L_{\mathrm{sub}} < L/2$, respectively [85].

Clifford simulation.—To support the theoretical predictions, we use QuantumClifford.jl package [105] to perform extensive large-scale Clifford simulations [106,107] where the random Clifford gates form a unitary 3-design [108]. We use the reset channel $\mathcal{R}_i(\rho) = \mathrm{tr}_i(\rho) \otimes |0\rangle\langle 0|_i$ to model the quantum noise, which is easy to implement in the current generation of quantum hardware [109,110], while our theoretical analysis does not depend on the choice of quantum channels. And we set the probability of projective measurement $0 < p_m < p_m^c$. The numerical results with quantum dephasing channels and $p_m > p_m^c$ can be found in SM [85].

The dynamics of mutual information $I_{AB:R}$ in the presence of temporally uncorrelated and correlated quantum noises are shown in Fig. 3 (see SM [85] for more numerical results for generic non-Markovian cases). The data with different system sizes and noise probabilities can be collapsed with rescaled time $t/q^{-1/2}$ and $t/q^{-2/3}$ for temporally uncorrelated and correlated quantum noises, consistent with the theoretical predictions. The fitting of the half-chain mutual information shown in the inset

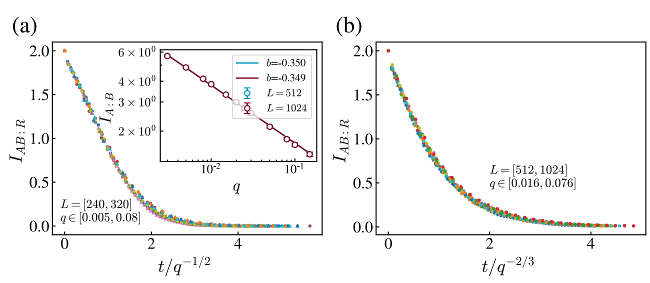

FIG. 3. The information protection dynamics. q represents the probability of reset channels and $p_m = 0.2 < p_m^c$ is the probability of projective measurement. (a) shows the mutual information $I_{AB:R}$ vs rescaled time $t/q^{-1/2}$ for temporally uncorrelated quantum noises. The inset shows the fitting of mutual information $I_{A:B}$ with the function $I_{A:B}(q) = aq^b$. b is very close to the theoretical prediction $-1/3$. (b) shows the mutual information $I_{AB:R}$ vs rescaled time $t/q^{-2/3}$ for temporally correlated quantum noises.

in Fig. 3(a) gives the $q^{-1/3}$ scaling. We have also demonstrated the scaling of von Neumann entropy [85].

Discussions and conclusion.—We provide a comprehensive analytical understanding of the impacts of quantum noises with different temporal correlations on entanglement generation and information protection: the mutual information satisfies the scaling $q^{-1/3}$ for both temporally uncorrelated and correlated noise, while the timescale of information protection for temporally uncorrelated and correlated noise is $q^{-1/2}$ and $q^{-2/3}$, respectively. These theoretical predictions are further demonstrated by convincing numerical results from Clifford circuit simulations [85].

It is worth noting that the information protection capacity of non-Markovian noise (temporally correlated) is much stronger than the Markovian noise case when q is small, which is consistent with recent studies on the unexpected benefits brought by non-Markovian noise in quantum simulation [111] and quantum computation [112]. In SM [85], we also investigated the information protection capacity for a general non-Markovian noise interpolating between the Markovian and the strongest non-Markovian limits in the no measurement limit. We found that the information protection timescale changes continuously from $q^{-1/2}$ in the Markovian limit to q^{-1} in the strong non-Markovian limit, consistent with the expectation.

Furthermore, our setup realizes the Hayden-Preskill protocol in hybrid quantum circuits by identifying the quantum noise channel (unitary evolution with ancilla qudits) as Hawking radiation through the ancilla qudits. The setup in this Letter overcomes the subtleties in the previous Hayden-Preskill analogy in hybrid quantum circuits [113]. By coupling the reference qudit to the system after reaching the steady state, i.e., the black hole with half of the qudits radiated out and maximally entangled with the environment, we recover the Hayden-Preskill thought experiment, in which Bob can successfully decode the information, and hence substantially reduce the mutual information between the black hole and Charlie with $O(1)$ more qubits radiated.

In conclusion, we have presented a comprehensive theoretical framework for understanding entanglement generation and information protection in noisy hybrid quantum circuits. This framework is applicable to both temporally uncorrelated (Markovian) and correlated (non-Markovian) quantum noises. This work not only reveals a thorough theoretical understanding of $q^{-1/3}$ scaling in the presence of quantum noises on MIPT setup but also highlights the distinctions between the effects on information protection of quantum noises with different temporal correlations which are indistinguishable from the entanglement perspective and initial state information protection protocol [85,114,115]. Furthermore, our theoretical analysis can be extended to the cases of quantum noises with system size-dependent probability, where MIPT still exists and a new noise-induced entanglement phase transition has been investigated [115].

This work is supported in part by the NSFC under Grant No. 11825404 (S. L., M. R. L.). S. L. and M. R. L. acknowledge the support from the Lavin-Bernick Grant during their visit to Tulane University, where part of the work was conducted. The work of S. K. J. is supported by a startup fund at Tulane University. S. X. Z. would like to acknowledge the helpful discussion with Yu-Qin Chen in terms of the non-Markovian noise.

*shixinzhang@tencent.com
†sjian@tulane.edu

[1] Y. Li, X. Chen, and M. P. A. Fisher, Quantum Zeno effect and the many-body entanglement transition, Phys. Rev. B **98**, 205136 (2018).
[2] Y. Li, X. Chen, and M. P. A. Fisher, Measurement-driven entanglement transition in hybrid quantum circuits, Phys. Rev. B **100**, 134306 (2019).
[3] B. Skinner, J. Ruhman, and A. Nahum, Measurement-induced phase transitions in the dynamics of entanglement, Phys. Rev. X **9**, 031009 (2019).
[4] M. Ippoliti and V. Khemani, Postselection-free entanglement dynamics via spacetime duality, Phys. Rev. Lett. **126**, 060501 (2021).
[5] T.-C. Lu and T. Grover, Spacetime duality between localization transitions and measurement-induced transitions, PRX Quantum **2**, 040319 (2021).
[6] M. Ippoliti, T. Rakovszky, and V. Khemani, Fractal, logarithmic, and volume-law entangled nonthermal steady states via spacetime duality, Phys. Rev. X **12**, 011045 (2022).
[7] M. J. Gullans and D. A. Huse, Dynamical purification phase transition induced by quantum measurements, Phys. Rev. X **10**, 041020 (2020).
[8] S. Choi, Y. Bao, X.-L. Qi, and E. Altman, Quantum error correction in scrambling dynamics and measurement-induced phase transition, Phys. Rev. Lett. **125**, 030505 (2020).
[9] A. Chan, R. M. Nandkishore, M. Pretko, and G. Smith, Unitary-projective entanglement dynamics, Phys. Rev. B **99**, 224307 (2019).
[10] M. Szyniszewski, A. Romito, and H. Schomerus, Entanglement transition from variable-strength weak measurements, Phys. Rev. B **100**, 064204 (2019).
[11] Y. Bao, S. Choi, and E. Altman, Theory of the phase transition in random unitary circuits with measurements, Phys. Rev. B **101**, 104301 (2020).
[12] R. Fan, S. Vijay, A. Vishwanath, and Y.-Z. You, Self-organized error correction in random unitary circuits with measurement, Phys. Rev. B **103**, 174309 (2021).
[13] Y. Li and M. P. A. Fisher, Statistical mechanics of quantum error correcting codes, Phys. Rev. B **103**, 104306 (2021).
[14] C.-M. Jian, Y.-Z. You, R. Vasseur, and A. W. W. Ludwig, Measurement-induced criticality in random quantum circuits, Phys. Rev. B **101**, 104302 (2020).

[15] E. V. H. Doggen, Y. Gefen, I. V. Gornyi, A. D. Mirlin, and D. G. Polyakov, Evolution of many-body systems under ancilla quantum measurements, Phys. Rev. B **107**, 214203 (2023).
[16] J. C. Hoke *et al.* (Google Quantum AI and Collaborators), Measurement-induced entanglement and teleportation on a noisy quantum processor, Nature (London) **622**, 481 (2023).
[17] Z.-C. Yang, Y. Li, M. P. A. Fisher, and X. Chen, Entanglement phase transitions in random stabilizer tensor networks, Phys. Rev. B **105**, 104306 (2022).
[18] X. Turkeshi, R. Fazio, and M. Dalmonte, Measurement-induced criticality in $(2+1)$-dimensional hybrid quantum circuits, Phys. Rev. B **102**, 014315 (2020).
[19] P. Sierant, M. Schirò, M. Lewenstein, and X. Turkeshi, Measurement-induced phase transitions in $(d+1)$-dimensional stabilizer circuits, Phys. Rev. B **106**, 214316 (2022).
[20] H. Liu, T. Zhou, and X. Chen, Measurement-induced entanglement transition in a two-dimensional shallow circuit, Phys. Rev. B **106**, 144311 (2022).
[21] X. Feng, B. Skinner, and A. Nahum, Measurement-induced phase transitions on dynamical quantum trees, PRX Quantum **4**, 030333 (2023).
[22] U. Agrawal, A. Zabalo, K. Chen, J. H. Wilson, A. C. Potter, J. H. Pixley, S. Gopalakrishnan, and R. Vasseur, Entanglement and charge-sharpening transitions in U(1) symmetric monitored quantum circuits, Phys. Rev. X **12**, 041002 (2022).
[23] H. Oshima and Y. Fuji, Charge fluctuation and charge-resolved entanglement in a monitored quantum circuit with $U(1)$ symmetry, Phys. Rev. B **107**, 014308 (2023).
[24] F. Barratt, U. Agrawal, S. Gopalakrishnan, D. A. Huse, R. Vasseur, and A. C. Potter, Field theory of charge sharpening in symmetric monitored quantum circuits, Phys. Rev. Lett. **129**, 120604 (2022).
[25] Y. Han and X. Chen, Entanglement dynamics in U(1) symmetric hybrid quantum automaton circuits, Quantum **7**, 1200 (2023).
[26] S. Majidy, U. Agrawal, S. Gopalakrishnan, A. C. Potter, R. Vasseur, and N. Y. Halpern, Critical phase and spin sharpening in SU(2)-symmetric monitored quantum circuits, Phys. Rev. B **108**, 054307 (2023).
[27] A. G. Moghaddam, K. Pöyhönen, and T. Ojanen, Exponential shortcut to measurement-induced entanglement phase transitions, Phys. Rev. Lett. **131**, 020401 (2023).
[28] S.-K. Jian, C. Liu, X. Chen, B. Swingle, and P. Zhang, Measurement-induced phase transition in the monitored Sachdev-Ye-Kitaev model, Phys. Rev. Lett. **127**, 140601 (2021).
[29] S. Sahu, S.-K. Jian, G. Bentsen, and B. Swingle, Entanglement phases in large-n hybrid Brownian circuits with long-range couplings, Phys. Rev. B **106**, 224305 (2022).
[30] S.-K. Jian and B. Swingle, Phase transition in von Neumann entanglement entropy from replica symmetry breaking, arXiv:2108.11973.
[31] A. Biella and M. Schiró, Many-body quantum Zeno effect and measurement-induced subradiance transition, Quantum **5**, 528 (2021).
[32] X. Turkeshi, A. Biella, R. Fazio, M. Dalmonte, and M. Schiró, Measurement-induced entanglement transitions in the quantum Ising chain: From infinite to zero clicks, Phys. Rev. B **103**, 224210 (2021).
[33] X. Turkeshi, M. Dalmonte, R. Fazio, and M. Schirò, Entanglement transitions from stochastic resetting of non-Hermitian quasiparticles, Phys. Rev. B **105**, L241114 (2022).
[34] X. Yu and X.-L. Qi, Measurement-induced entanglement phase transition in random bilocal circuits, arXiv:2201.12704.
[35] A. Nahum, S. Roy, B. Skinner, and J. Ruhman, Measurement and entanglement phase transitions in all-to-all quantum circuits, on quantum trees, and in Landau-Ginsburg theory, PRX Quantum **2**, 010352 (2021).
[36] P. Sierant, G. Chiriacò, F. M. Surace, S. Sharma, X. Turkeshi, M. Dalmonte, R. Fazio, and G. Pagano, Dissipative Floquet dynamics: From steady state to measurement induced criticality in trapped-ion chains, Quantum **6**, 638 (2022).
[37] G. S. Bentsen, S. Sahu, and B. Swingle, Measurement-induced purification in large-n hybrid Brownian circuits, Phys. Rev. B **104**, 094304 (2021).
[38] T. Müller, S. Diehl, and M. Buchhold, Measurement-induced dark state phase transitions in long-ranged fermion systems, Phys. Rev. Lett. **128**, 010605 (2022).
[39] M. Block, Y. Bao, S. Choi, E. Altman, and N. Y. Yao, Measurement-induced transition in long-range interacting quantum circuits, Phys. Rev. Lett. **128**, 010604 (2022).
[40] T. Hashizume, G. Bentsen, and A. J. Daley, Measurement-induced phase transitions in sparse nonlocal scramblers, Phys. Rev. Res. **4**, 013174 (2022).
[41] T. Minato, K. Sugimoto, T. Kuwahara, and K. Saito, Fate of measurement-induced phase transition in long-range interactions, Phys. Rev. Lett. **128**, 010603 (2022).
[42] S. Sharma, X. Turkeshi, R. Fazio, and M. Dalmonte, Measurement-induced criticality in extended and long-range unitary circuits, SciPost Phys. Core **5**, 023 (2022).
[43] P. Zhang, C. Liu, S.-K. Jian, and X. Chen, Universal entanglement transitions of free fermions with long-range non-unitary dynamics, Quantum **6**, 723 (2022).
[44] V. Ravindranath, Y. Han, Z.-C. Yang, and X. Chen, Entanglement steering in adaptive circuits with feedback, Phys. Rev. B **108**, L041103 (2023).
[45] V. Ravindranath, Z.-C. Yang, and X. Chen, Free fermions under adaptive quantum dynamics, arXiv:2306.16595.
[46] N. O'Dea, A. Morningstar, S. Gopalakrishnan, and V. Khemani, Entanglement and absorbing-state transitions in interactive quantum dynamics, Phys. Rev. B **109**, L020304 (2024).
[47] P. Sierant and X. Turkeshi, Controlling entanglement at absorbing state phase transitions in random circuits, Phys. Rev. Lett. **130**, 120402 (2023).
[48] S. P. Kelly and J. Marino, Generalizing measurement-induced phase transitions to information exchange symmetry breaking, arXiv:2402.13271.
[49] S. P. Kelly and J. Marino, Information exchange symmetry breaking in quantum-enhanced experiments, arXiv:2310.03061.
[50] M. Tsitsishvili, D. Poletti, M. Dalmonte, and G. Chiriacò, Measurement induced transitions in non-Markovian free fermion ladders, SciPost Phys. Core **7**, 011 (2024).

[51] G. Chiriacò, M. Tsitsishvili, D. Poletti, R. Fazio, and M. Dalmonte, Diagrammatic method for many-body non-Markovian dynamics: Memory effects and entanglement transitions, Phys. Rev. B **108**, 075151 (2023).

[52] E. V. Doggen, I. V. Gornyi, and A. D. Mirlin, Ancilla quantum measurements on interacting chains: Sensitivity of entanglement dynamics to the type and concentration of detectors, arXiv:2311.13011.

[53] H. Kim and D. A. Huse, Ballistic spreading of entanglement in a diffusive nonintegrable system, Phys. Rev. Lett. **111**, 127205 (2013).

[54] A. Nahum, J. Ruhman, S. Vijay, and J. Haah, Quantum entanglement growth under random unitary dynamics, Phys. Rev. X **7**, 031016 (2017).

[55] M. Ippoliti, M. J. Gullans, S. Gopalakrishnan, D. A. Huse, and V. Khemani, Entanglement phase transitions in measurement-only dynamics, Phys. Rev. X **11**, 011030 (2021).

[56] C. Noel, P. Niroula, D. Zhu, A. Risinger, L. Egan, D. Biswas, M. Cetina, A. V. Gorshkov, M. J. Gullans, D. A. Huse, and C. Monroe, Measurement-induced quantum phases realized in a trapped-ion quantum computer, Nat. Phys. **18**, 760 (2022).

[57] Y. Bao, S. Choi, and E. Altman, Symmetry enriched phases of quantum circuits, Ann. Phys. (Amsterdam) **435**, 168618 (2021).

[58] B. C. Dias, D. Perkovic, M. Haque, P. Ribeiro, and P. A. McClarty, Quantum noise as a symmetry-breaking field, Phys. Rev. B **108**, L060302 (2023).

[59] S.-K. Jian, C. Liu, X. Chen, B. Swingle, and P. Zhang, Quantum error as an emergent magnetic field, arXiv: 2106.09635.

[60] Y. Li and M. Claassen, Statistical mechanics of monitored dissipative random circuits, Phys. Rev. B **108**, 104310 (2023).

[61] Z. Li, S. Sang, and T. H. Hsieh, Entanglement dynamics of noisy random circuits, Phys. Rev. B **107**, 014307 (2023).

[62] S. Liu, M.-R. Li, S.-X. Zhang, S.-K. Jian, and H. Yao, Universal Kardar-Parisi-Zhang scaling in noisy hybrid quantum circuits, Phys. Rev. B **107**, L201113 (2023).

[63] A. Zabalo, J. H. Wilson, M. J. Gullans, R. Vasseur, S. Gopalakrishnan, D. A. Huse, and J. H. Pixley, Infinite-randomness criticality in monitored quantum dynamics with static disorder, Phys. Rev. B **107**, L220204 (2023).

[64] G. Shkolnik, A. Zabalo, R. Vasseur, D. A. Huse, J. H. Pixley, and S. Gazit, Measurement induced criticality in quasiperiodic modulated random hybrid circuits, Phys. Rev. B **108**, 184204 (2023).

[65] H.-P. Breuer, E.-M. Laine, J. Piilo, and B. Vacchini, Colloquium: Non-Markovian dynamics in open quantum systems, Rev. Mod. Phys. **88**, 021002 (2016).

[66] Z. Cai, R. Babbush, S. C. Benjamin, S. Endo, W. J. Huggins, Y. Li, J. R. McClean, and T. E. O'Brien, Quantum error mitigation, Rev. Mod. Phys. **95**, 045005 (2023).

[67] K. Temme, S. Bravyi, and J. M. Gambetta, Error mitigation for short-depth quantum circuits, Phys. Rev. Lett. **119**, 180509 (2017).

[68] Y. Kim, C. J. Wood, T. J. Yoder, S. T. Merkel, J. M. Gambetta, K. Temme, and A. Kandala, Scalable error mitigation for noisy quantum circuits produces competitive expectation values, Nat. Phys. **19**, 752 (2023).

[69] S. Zhang, Z.-Q. Wan, C.-Y. Hsieh, H. Yao, and S. Zhang, Variational quantumneural hybrid error mitigation, Adv. Quantum Technol. **6**, 2300147 (2023).

[70] Y. Kim, A. Eddins, S. Anand, K. X. Wei, E. van den Berg, S. Rosenblatt, H. Nayfeh, Y. Wu, M. Zaletel, K. Temme, and A. Kandala, Evidence for the utility of quantum computing before fault tolerance, Nature (London) **618**, 500 (2023).

[71] C. H. Bennett, D. P. DiVincenzo, J. A. Smolin, and W. K. Wootters, Mixed-state entanglement and quantum error correction, Phys. Rev. A **54**, 3824 (1996).

[72] M. Horodecki, P. Horodecki, and R. Horodecki, Mixed-state entanglement and distillation: Is there a "bound" entanglement in nature?, Phys. Rev. Lett. **80**, 5239 (1998).

[73] M. A. Nielsen and I. L. Chuang, *Quantum Computation and Quantum Information* (Cambridge University Press, Cambridge, England, 2010).

[74] G. Vidal and R. F. Werner, Computable measure of entanglement, Phys. Rev. A **65**, 032314 (2002).

[75] M. B. Plenio, Logarithmic negativity: A full entanglement monotone that is not convex, Phys. Rev. Lett. **95**, 090503 (2005).

[76] P. Calabrese, J. Cardy, and E. Tonni, Entanglement negativity in quantum field theory, Phys. Rev. Lett. **109**, 130502 (2012).

[77] P. Calabrese, J. Cardy, and E. Tonni, Entanglement negativity in extended systems: A field theoretical approach, J. Stat. Mech. (2013) P02008.

[78] T.-C. Lu and T. Grover, Singularity in entanglement negativity across finite-temperature phase transitions, Phys. Rev. B **99**, 075157 (2019).

[79] T.-C. Lu, T. H. Hsieh, and T. Grover, Detecting topological order at finite temperature using entanglement negativity, Phys. Rev. Lett. **125**, 116801 (2020).

[80] T.-C. Lu and T. Grover, Entanglement transitions as a probe of quasiparticles and quantum thermalization, Phys. Rev. B **102**, 235110 (2020).

[81] K.-H. Wu, T.-C. Lu, C.-M. Chung, Y.-J. Kao, and T. Grover, Entanglement Renyi negativity across a finite temperature transition: A Monte Carlo study, Phys. Rev. Lett. **125**, 140603 (2020).

[82] S. Sang, Y. Li, T. Zhou, X. Chen, T. H. Hsieh, and M. P. Fisher, Entanglement negativity at measurement-induced criticality, PRX Quantum **2**, 030313 (2021).

[83] H. Shapourian, S. Liu, J. Kudler-Flam, and A. Vishwanath, Entanglement negativity spectrum of random mixed states: A diagrammatic approach, PRX Quantum **2**, 030347 (2021).

[84] Z. Weinstein, Y. Bao, and E. Altman, Measurement-induced power-law negativity in an open monitored quantum circuit, Phys. Rev. Lett. **129**, 080501 (2022).

[85] See Supplemental Material at http://link.aps.org/supplemental/10.1103/PhysRevLett.132.240402 for more details, including (i) the introduction to the effective statistical model, (ii) the analytical understanding in the presence of temporally uncorrelated quantum noises, (iii) the analytical understanding in the presence of temporally correlated quantum noises, (iv) numerical results for

larger measurement rate $p_m > p_m^c$, (v) information protection with other setups, (vi) connection between information protection and time correlation of quantum noises, (vii) details of numerical simulation, and Refs. [86–91].

[86] T. Zhou and A. Nahum, Emergent statistical mechanics of entanglement in random unitary circuits, Phys. Rev. B **99**, 174205 (2019).

[87] B. Collins, Moments and cumulants of polynomial random variables on unitarygroups, the Itzykson-Zuber integral, and free probability, Int. Math. Res. Not. **2003**, 953 (2003).

[88] B. Collins and P. Śniady, Integration with respect to the Haar measure on unitary, orthogonal and symplectic group, Commun. Math. Phys. **264**, 773 (2006).

[89] A. Nahum, S. Vijay, and J. Haah, Operator spreading in random unitary circuits, Phys. Rev. X **8**, 021014 (2018).

[90] M. Huang, M. E. Fisher, and R. Lipowsky, Wetting in a two-dimensional random-bond Ising model, Phys. Rev. B **39**, 2632 (1989).

[91] Y.-Q. Chen, S. Liu, and S.-X. Zhang, Subsystem information capacity in random circuits and Hamiltonian dynamics, arXiv:2405.05076.

[92] M. Kardar, G. Parisi, and Y.-C. Zhang, Dynamic scaling of growing interfaces, Phys. Rev. Lett. **56**, 889 (1986).

[93] M. Kardar, Roughening by impurities at finite temperatures, Phys. Rev. Lett. **55**, 2923 (1985).

[94] D. A. Huse, C. L. Henley, and D. S. Fisher, Huse, Henley, and Fisher respond, Phys. Rev. Lett. **55**, 2924 (1985).

[95] E. Medina, T. Hwa, M. Kardar, and Y.-C. Zhang, Burgers equation with correlated noise: Renormalization-group analysis and applications to directed polymers and interface growth, Phys. Rev. A **39**, 3053 (1989).

[96] T. Gueudré and P. L. Doussal, Directed polymer near a hard wall and KPZ equation in the half-space, Europhys. Lett. **100**, 26006 (2012).

[97] G. Barraquand, A. Krajenbrink, and P. Le Doussal, Half-space stationary Kardar–Parisi–Zhang equation, J. Stat. Phys. **181**, 1149 (2020).

[98] P. Hayden and J. Preskill, Black holes as mirrors: Quantum information in random subsystems, J. High Energy Phys. 09 (2007) 120.

[99] A. A. Mele, A. Angrisani, S. Ghosh, S. Khatri, J. Eisert, D. S. França, and Y. Quek, Noise-induced shallow circuits and absence of barren plateaus, arXiv:2403.13927.

[100] We note that the time required to reach the steady state in the noisy hybrid quantum circuits is $O(q^{-1})$ and size-independent, regardless of the temporal correlation of quantum noises, arising from the competition between the spin configuration where all the spins are fixed to $\mathbb{C}$ with free energy $O(qLt)$ and the spin configuration with domain wall where the leading term of free energy is $O(L)$.

[101] H. Nishimori, *Statistical Physics of Spin Glasses and Information Processing: An Introduction* (Clarendon Press, Oxford, 2001), p. 111.

[102] M. Kardar, *Statistical Physics of Fields* (Cambridge University Press, Cambridge, England, 2007).

[103] X. Dong, X.-L. Qi, and M. Walter, Holographic entanglement negativity and replica symmetry breaking, J. High Energy Phys. 06 (2021) 024.

[104] Y. Li, S. Vijay, and M. P. Fisher, Entanglement domain walls in monitored quantum circuits and the directed polymer in a random environment, PRX Quantum **4**, 010331 (2023).

[105] Stefan Krastanov, QuantumClifford.jl (2019), https://github.com/QuantumSavory/QuantumClifford.jl.

[106] S. Aaronson and D. Gottesman, Improved simulation of stabilizer circuits, Phys. Rev. A **70**, 052328 (2004).

[107] M. A. Nielsen, I. Chuang, and L. K. Grover, Quantum computation and quantum information, Am. J. Phys. **70**, 558 (2002).

[108] Z. Webb, The Clifford group forms a unitary 3-design, Quantum Inf. Comput. **16**, 1379 (2016).

[109] Y. Zhou, Z. Zhang, Z. Yin, S. Huai, X. Gu, X. Xu, J. Allcock, F. Liu, G. Xi, Q. Yu, H. Zhang, M. Zhang, H. Li, X. Song, Z. Wang, D. Zheng, S. An, Y. Zheng, and S. Zhang, Rapid and unconditional parametric reset protocol for tunable superconducting qubits, Nat. Commun. **12**, 5924 (2021).

[110] K. Geerlings, Z. Leghtas, I. M. Pop, S. Shankar, L. Frunzio, R. J. Schoelkopf, M. Mirrahimi, and M. H. Devoret, Demonstrating a driven reset protocol for a superconducting qubit, Phys. Rev. Lett. **110**, 120501 (2013).

[111] Y.-Q. Chen, S.-X. Zhang, and S. Zhang, Non-Markovianity benefits quantum dynamics simulation, arXiv:2311.17622.

[112] J. Kattemölle and G. Burkard, Ability of error correlations to improve the performance of variational quantum algorithms, Phys. Rev. A **107**, 042426 (2023).

[113] Z. Weinstein, S. P. Kelly, J. Marino, and E. Altman, Scrambling transition in a radiative random unitary circuit, Phys. Rev. Lett. **131**, 220404 (2023).

[114] I. Lovas, U. Agrawal, and S. Vijay, Quantum coding transitions in the presence of boundary dissipation, arXiv:2304.02664.

[115] S. Liu, M.-R. Li, S.-X. Zhang, S.-K. Jian, and H. Yao, Noise-induced phase transitions in hybrid quantum circuits, arXiv:2401.16631.